Electronic properties and spin polarization in coupled quantum dots

Satyadev Nagaraja and Jean-Pierre Leburton
Beckman Institute for Advanced Science & Technology, 405 N. Mathews Avenue, Urbana, Illinois 61820
and Department of Electrical and Computer Engineering, University of Illinois at Urbana-Champaign, Urbana, Illinois 61820

Richard M. Martin
Beckman Institute for Advanced Science & Technology, 405 N. Mathews Avenue, Urbana, Illinois 61820
and Department of Physics, University of Illinois at Urbana-Champaign, Urbana, Illinois 61801
(Received 14 December 1998; revised manuscript received 28 April 1999)

Electronic structure and charging properties of an electrostatically defined double quantum dot system are investigated within the local spin density approximation under the density functional theory. Characteristics of electron charging of the double dot system is influenced by quantum-mechanical as well as electrostatic coupling between the individual dots. In the case of weak coupling, the double dot system is shown to exhibit double electron charging in agreement with the observations of Waugh *et al.* [Phys. Rev. Lett. **75**, 705 (1995)]. Also, the coupled dot system shows spin polarization for higher number of electrons in the dot N due to Hund's rule. For strong coupling, we show that coherent *bonding* and *antibonding* states are formed which produce a reordering of the single-particle energy levels and revert the double dot system into a spin unpolarized state for same N. [S0163-1829(99)05435-1]

I. INTRODUCTION

Physical properties such as three-dimensional electron confinement, energy quantization, and shell structures, typical of atoms, can now be realized in ultrasmall semiconductor structures called quantum dots (QD's). The ability to observe such atomic phenomena that occur naturally on the scale of a few Å in manmade nanostructures with feature size of a few hundreds or thousands of angstroms has resulted in a flurry of experimental and theoretical investigations of QDs in recent years. Motivation for such studies has risen largely from a need to study fundamental electronic properties, but also increasingly from the possibility of making ultrasmall memories[1] and high efficiency lasers.[2] Lately, attention has been focussed on arrays of quantum dots coupled through tunnel junctions.[3–5] Their appeal stems form the many features they share with molecules. Just as in molecules electron states can couple forming covalent states that are delocalized over the entire array making possible for an occupying electron to tunnel between the various dots without being localized to any.[6,7] These *bonding states* are lower in energy than the constituent dot states by an amount that is equivalent to the binding energy of the molecule. Hence a two-dot system may be compared to a diatomic molecule. Such artificial molecules provide an advantage in that the number of electrons in the coupled dot, equivalently the constituent ''atoms'' in the periodic table, may be varied by varying an external potential. Different molecular analogs can be realized by varying the size of the dots, simultaneously or independently, and their number of electrons. Furthermore, the vibrational motion of a molecule may be simulated by driving such an array between weak and strong tunneling regimes.

The volume of experimental[8,9,4] and theoretical work[3,10–14] on coupled dots has been growing in recent times. In particular, Ruzin *et al.*[11] studied the Coulomb blockade structure for two nonidentical dots using the activation-energy approach. Stafford *et al.*[12] and Klimeck *et al.*[13] have used a Mott-Hubbard approach with and without interdot capacitances to determine the many-body wave function for an array of dots. More recently Golden *et al.*[14] have studied the problem of Coulomb blockade peak splitting in the weak and strong coupling limits to explain the experimental data in Ref. 5. The present work is motivated by the following factors.

(1) The need to treat the problem self-consistently since the distortion of the confining potential and the weakening of confinement are both significant as the charge in the dot increases.[15,16] The latter effect is particularly critical in electrostatically confined dots.

(2) The need to consider explicitly the electron spin. This is necessitated by the findings of Tarucha *et al.* in gated vertical quantum dots which established that shell filling in QDs is governed by Hund's rules just as in atoms. Some recent theoritical investigations of Lee *et al.*,[17] Fonseca *et al.*,[18] Wojs *et al.*,[19] and Koskinen *et al.*[20] have studied spin effects in LSDA in single QDs. To our knowledge, rigorous calculations based on a spin dependent model of double QDs have not been done so far.

(3) The experimental results of Waugh *et al.*[5] on the conductance of electrostatically confined double and triple dots in the weak and strong tunneling regimes. The splitting of conductance peaks that increased with the interdot tunneling strength coupling, establishes the fact that the splitting is proportional to the energy of interaction between the dots. Another feature though weak but clearly visible in their results [Figs. 2(a), 2(b), and 2(c) in Ref. 5] is the increase in the separation of the successive split peaks for a constant tunnel conductance.

In the present work, we focus on a system of two similar dots whose dimensions are such that the electron-electron interaction energy is comparable to the single-particle energy level spacing ΔE. The number of electrons in the dot, N, is

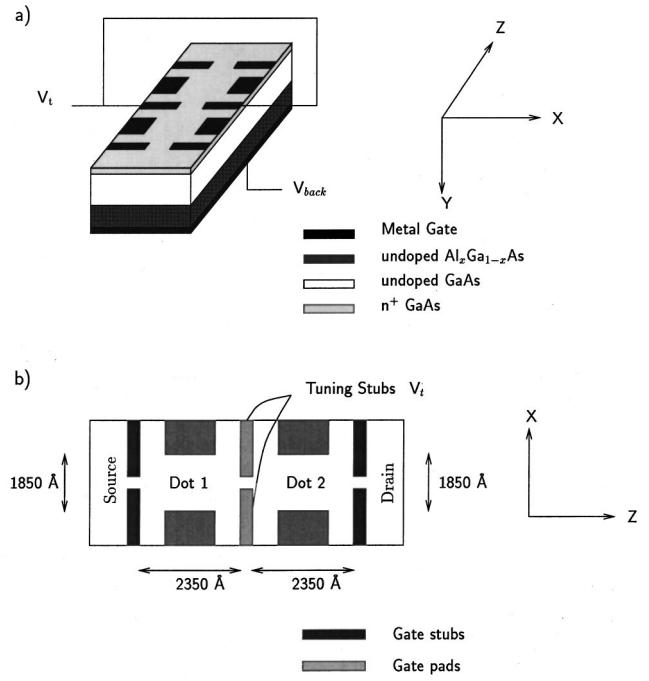

FIG. 1. The double dot system. (a) Layer structure of the double dot, (b) Schematic representation along the *x*-*z* plane. The gate stub voltage$=-1.2$ V; gate pad voltage$=-0.40$ V.

restricted to very low values, a situation comparable to a light molecule such as H-H or Be-Be. We investigate the electronic properties of the coupled-dot system by solving self-consistently the Schrödinger and Poisson equations on a three dimensional grid. The electron spin has been considered explicitly under the local spin density approximation (LSDA) in the density functional theory.[21] From our investigations we find that in the weak tunneling regime, charging of the two dots can occur simultaneously, but as N increases this simultaneous charging is terminated because of the increase in the Coulomb repulsion energy. We also find that for eight-electrons in the double-dot—a situation similar to a Be-Be molecule—the ground state of the system is spin polarized in the weak tunneling regime while it is unpolarized in the strong tunneling regime.

In the following section we state the motivations and scope of the present work. In Sec. II we describe the dot structure. In Sec. III we describe briefly the methods used to solve the Schrödinger and Poisson equations, and the criterion used to determine the charge degeneracy points. In Sec. IV we present our results on the electronic properties of the system and show qualitative agreements with the experiments of Waugh *et al.*[5] We also show that for weak interdot coupling with eight electrons in the artificial diatomic molecule, the system favors a spin polarized state which reverts to an unpolarized state as the coupling is increased. Finally, in Sec. V we summarize our findings.

II. DOT STRUCTURES

The layered structure, shown in Fig. 1(a), consists of an inverted GaAs/$Al_{0.3}Ga_{0.7}As$ heterostructure which confines the electrons to a 2D gas at the interface. In our model, the simulated structure consists of a 22.5-nm layer of undoped $Al_{0.3}Ga_{0.7}As$ followed by a 125-nm layer of undoped GaAs and finally an 18 nm GaAs cap layer. The cap layer is uniformly doped to $5\times10^{18}\text{cm}^{-3}$ so that the conduction band edge is just above the Fermi level at the GaAs-cap layer-undoped GaAs boundary. The inverted heterostructure is grown on a GaAs substrate and charge control is achieved by varying the voltage on the back gate V_{back}. We assume a negligible voltage drop across the substrate, hence we apply V_{back} directly to the bottom of the $Al_{0.3}Ga_{0.7}As$ layer. The two dots are defined by energizing the ten metallic gates shown in Fig. 1(b), with the coupling between them varied by means of the voltage V_t on the tuning gates. Electron charging of the two dots is possible through tunnel injection from the adjacent two-dimensional regions through the 35-nm opening between the opposite stubs.

III. MODEL

We solve the single-particle effective-mass Schrödinger and Poisson equations self-consistently in the entire dot structure. The Schrödinger equation is three dimensional in the central double-dot region and one dimensional in the adjacent source and drain. The many-body effects are included under the spin-dependent LSDA. This method, which is an improvement over the previous spin independent LDA approaches,[16,22–24] has been used successfully to investigate spin dependent effects in QDs such as Hund's rules in shell filling.[17,18] Hence the implementation of a spin-dependent scheme involves solution of the Schrödinger equation twice—once for each of the spins, up ($\uparrow$) and down ($\downarrow$). The respective Hamiltonians are identical in all respects except for the exchange-correlation potential $\mu_{\text{xc}}^{\uparrow(\downarrow)}$ which as parametrized by Ceperley and Alder[25] is given by

$$\mu_{\text{xc}}^{\uparrow(\downarrow)}=\frac{d(n\epsilon_{\text{xc}}[n,\zeta])}{dn^{\uparrow(\downarrow)}}, \tag{1}$$

where $\epsilon_{\text{xc}}[n,\zeta]$ is the exchange-correlation energy as a function of the total electron density $n(\mathbf{r})$ $[=n^{\uparrow}(\mathbf{r})+n^{\downarrow}(\mathbf{r})]$ and the fractional spin polarization $\zeta=(n^{\uparrow}-n^{\downarrow})/n$. The exchange portion of $\epsilon_{\text{xc}}[n,\zeta]$ is simply a sum of terms for up and down spins

$$\epsilon_x[n,\zeta]=-\frac{3}{4}\left(\frac{3}{\pi}n(\mathbf{r})\right)^{1/3}[1+f(\zeta)], \tag{2}$$

where

$$f(\zeta)=\frac{(1+\zeta)^{4/3}+(1-\zeta)^{4/3}-2}{2}. \tag{3}$$

The correlation term is calculated using the same parametrization as the LDA (Ref. 16) but interpolating between the results of a spin-polarized and unpolarized free electron gas[26] depending on the spin polarization in the dot.

Therefore, the Hamiltonian $H^{\uparrow(\downarrow)}$ for the spin $\uparrow(\downarrow)$ electrons,

$$\hat{H}^{\uparrow(\downarrow)}=-\frac{\hbar^2}{2}\nabla\left[\frac{1}{m^*(\mathbf{r})}\nabla\right]+E_c(\mathbf{r})+\mu_{\text{xc}}^{\uparrow(\downarrow)}[n], \tag{4}$$

where $m^*(\mathbf{r})$ is the position dependent effective mass of the electron in the different materials, $E_c(\mathbf{r})=\phi(\mathbf{r})+\Delta E_{os}$, is the effective conduction band edge, where $\phi(\mathbf{r})$ is the electrostatic potential, ΔE_{os} is the conduction band offset. The 3D Poisson equation for the electrostatic potential $\phi(\mathbf{r})$ reads

$$\nabla[\epsilon(\mathbf{r})\nabla\phi(\mathbf{r})]=-\rho(\mathbf{r}), \tag{5}$$

where the charge density $\rho(\mathbf{r})$ is given by $e[p(\mathbf{r})-n(\mathbf{r})+N_D^+(\mathbf{r})-N_A^-(\mathbf{r})]$. Here, $\epsilon(\mathbf{r})$ is the permittivity of the material and is a function of $y-$ only throughout this work, $p(\mathbf{r})$ is the hole concentration, $n(\mathbf{r})$, the total electron concentration and $N_D^+(\mathbf{r})$ and $N_A^-(\mathbf{r})$ are the ionized donor and acceptor concentrations, respectively. $N_D^+(\mathbf{r})$ is relevant only in the region outside the quantum dot—the dot region itself being undoped or very slightly *p* doped—and is a function of the position of the Fermi level with respect to the conduction band. $N_A^-(\mathbf{r})$ is neglected as we have only *n*-type regions in our structure. In reality, though, the undoped regions usually contain a residual acceptor concentration of about $10^{15}\mathrm{cm}^{-3}$ when structures are grown by molecular beam epitaxy (MBE). However, this can be neglected as it is many orders of magnitute smaller than the electron densities encountered in this problem. For similar reasons, the hole density $p(\mathbf{r})$ may also be neglected. The electron concentrations for each spin in the dot are calculated from the wave functions obtained from the respective Schrödinger equations, i.e., $n^{\uparrow(\downarrow)}(\mathbf{r})=\Sigma_i|\psi_i^{\uparrow(\downarrow)}(\mathbf{r})|^2$, while for the region outside the dot a Thomas-Fermi distribution is used, i.e., the electron density is locally a function of the position of the Fermi level with respect to the conduction band edge as opposed to those in the dot which are calculated from the occupation of the quantized 0D eigenstates. The relevant expressions for $n(\mathbf{r})$ and N_D^+ may be found in Ref. 27.

The various gate voltages—V_{back}, V_t and those on the metallic pads and stubs—determine the boundary conditions for the Poisson equation. Specifically, Dirichlet conditions are imposed on the top and bottom surfaces of the dot structure by defining the potential $\phi(\mathbf{r})$ to be $\phi_m(\mathbf{r})+V_{\mathrm{ext}}$, where $\phi_m(\mathbf{r})$ denotes the Fermi level pinning at the semiconductor surface and V_{ext} the external gate potential. For the lateral surfaces (*xy* plane in Fig. 1) vanishing electric fields are assumed. This is justified by the fact that these lateral boundary surfaces are far enough from the dot for the electric fields to have vanished.

Solution of the Schrödinger and Poisson equations proceeds by solving the Schrödinger for both spins, calculating the respective electron densities and exchange correlation potentials, solving the Poisson equation to determine the potential $\phi(\mathbf{r})$ and repeating the sequence until the convergence criterion is satisfied. This occurs when the maximum difference in eigenenergies between two successive iterations (for both spins) is less than 10^{-6} eV, and the global residual of the Poisson's equation, the difference between the right and left hand terms of Eq. (5) summed over all grid points, is less than 10^5 $\mathrm{V\,cm}^{-2}$. The latter criterion results in a potential whose variation between successive iterations is less than 10^{-6} V, which is of sufficient accuracy as it is much lower than $k_BT(=2\times10^{-5}$ eV).

The Schrödinger equation is solved using the iterative extraction orthogonalization method (IEOM), wherein a functional of the Hamiltonian is applied to a guess eigenstate iteratively to extract the ground state of the operator.[22] Higher states are extracted by repeating the procedure for several initial guess states and orthogonalizing all the resulting states after each iteration of the Schrödinger equation. The Poisson equation is solved by combining a Newton's technique with successive over relaxation method. The main advantage of using this method is that an arbitrary number of eigenstates can be obtained without involving huge computation time and memory resources.

Single-electron charging. A QD system that is in diffusive isolation from its environment contains an integer number of electrons at equilibrium. The exact number N_{eq}, for a given external potential minimizes the total energy of the system. Electrostatically confined dots, like the present one, cannot be in diffusive isolation since they have to be connected to their outside environment to facilitate charge injection into the system. However, at low temperature and low N_{eq} the electrons occupy the lowest single particle states which are well confined to the dot thereby achieving diffusive isolation.

The determination of N_{eq} can be done by minimizing the Gibbs free energy $F(N)$ for various values of N.[16] This requires the computation of the partition function $Z(N)$ from the grand canonical ensemble for the whole system, i.e., electrons and their environment—a computationally expensive method. Due to its elegance and simplicity in implementation we prefer to use Slater's transition rule[28]

$$E_T(N+1)-E_T(N)=\int_0^1\epsilon_{\mathrm{LAO}}(n)dn\simeq\epsilon_{\mathrm{LAO}}\left(\frac{1}{2}\right), \tag{6}$$

where $E_T(N)$ is the total energy of the dot for N electrons and ϵ_{LAO} is the lowest available orbital. The above equation gives the addition energy, i.e. the energy required to add an electron to a dot containing N electrons, in terms of a transition state which is defined as a state containing $N+0.5$ electrons. While the N electrons occupy the lowest N single particle states, the 0.5 electron occupies the lowest available single particle state ϵ_{LAO}. N_{eq} is determined by whether $\epsilon_{\mathrm{LAO}}(\frac{1}{2})$ is positive ($N_{eq}=N$) or negative ($N_{eq}=N+1$). The $N\rightarrow N+1$ transition points are determined by populating the system with $N+0.5$ electrons and varying V_{back} until $\epsilon_{\mathrm{LAO}}(\frac{1}{2})$ is just negative. It must be noted that the approximation made in Eq. (6) is valid only if ϵ_{LAO} varies linearly with N. Calculations of Fonseca *et al.*[18] have established the validity of the approximation in self-assembled quantum dots.

IV. RESULTS

Figure 2(a) shows the total electrostatic potential for the empty double-dot in the plane of the hetero-interface for $V_t=-0.67$ V. The two dot regions are visible as depressions in the region 4000 Å $\leqslant z\leqslant$ 8000 Å and 2500 Å $\leqslant x\leqslant$ 4200 Å. The potential in the dots are parabolic at low energy as seen more clearly in Fig. 2(b), which shows the potential along *z*, the direction of coupling of the two dots for two values of V_t. For $V_t=-0.67$ V, therafter referred to as the weak-coupling regime, the interdot barrier (Δ_{67} in Fig. 2) is 4 meV, while for $V_t=-0.60$ V, i.e., the strong coupling re-

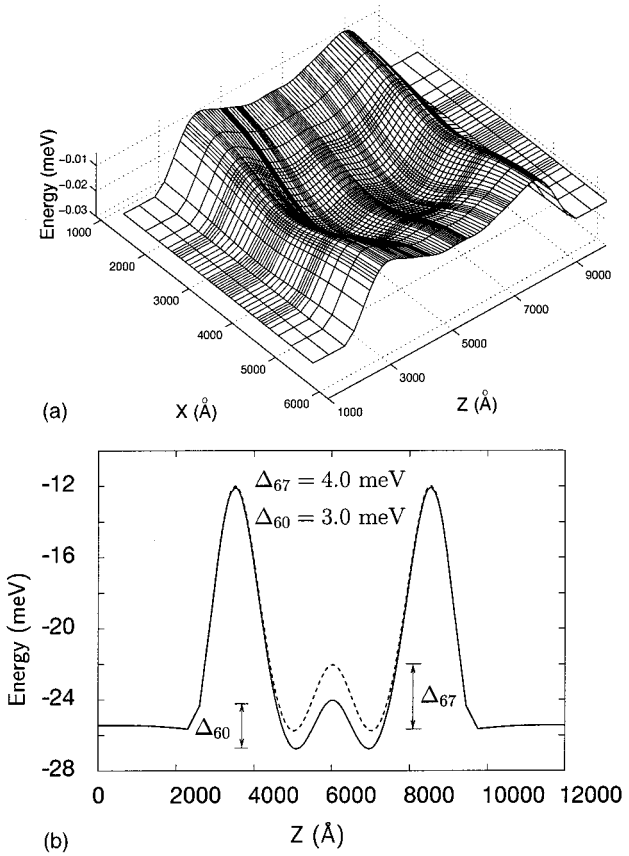

FIG. 2. Potential profile for the empty double dot (a) in the plane of the heterointerface (b) along z in the weak (dashed line), $V_t = -0.67$ V, and strong (solid line), $V_t = -0.60$ V, coupling regimes. The corresponding interdot barriers, Δ_{67} and Δ_{60}, are seen to be 4 and 3 meV, respectively.

gime, the interdot barrier (Δ_{60} in Fig. 2) is reduced to 3 meV. The entire double-dot, as seen, is bounded by 14 meV tunnel barriers at the source and drain ends. Confinement along the vertical, y, direction is provided by a combination of the band offset of 255 meV between the GaAs and $Al_{0.3}Ga_{0.7}As$ and a large vertical electrostatic field, $F_y \simeq 35$ kV/cm, in GaAs. This results in the separation between energy levels along y of 30–40 meV, much greater than that in the x-z plane which is of the order of 1 meV. This large level separation results in only the ground state (along the y direction) to be occupied at low temperatures. All the results present correspond to $T = 0.25$ K.

Figure 3 shows the schematic of the lowest four states with their wave functions in the double dot for $V_t = -0.67$ V and $V_t = -0.60$ V. For both values of V_t the ground state in the individual dots is 1s type, and form a degenerate pair. However, the first excited states, which are p_x and p_z like, are degenerate for weak coupling, i.e., $V_t = -0.67$ V, whereas for strong coupling ($V_t = -0.60$ V), the p_z-like states couple to form symmetric (bonding) and antisymmetric (antibonding) states which are lower in energy than the p_x-like states as seen in Fig. 3. This reordering of the states has an important bearing on the spin-polarization of the double-dot system, as shall be fully explained later.

Figure 4(a) shows the *Coulomb staircase* indicating the variation of the number of electrons in the dot with V_{back} at $V_t = -0.67$ V. For $V_{\text{back}} = 0.9769$ V, $\epsilon_{\text{LAO}}(0.5)$ is just negative, implying that the dot can accept one electron in the lowermost 1s state. At this point no distinction is made as to whether dot 1 or dot 2 or both are occupied since, in our model, the two dots are identical from the electrostatic and quantum mechanical points of view. The dots are decoupled quantum mechanically since the leakage of the 1s wave

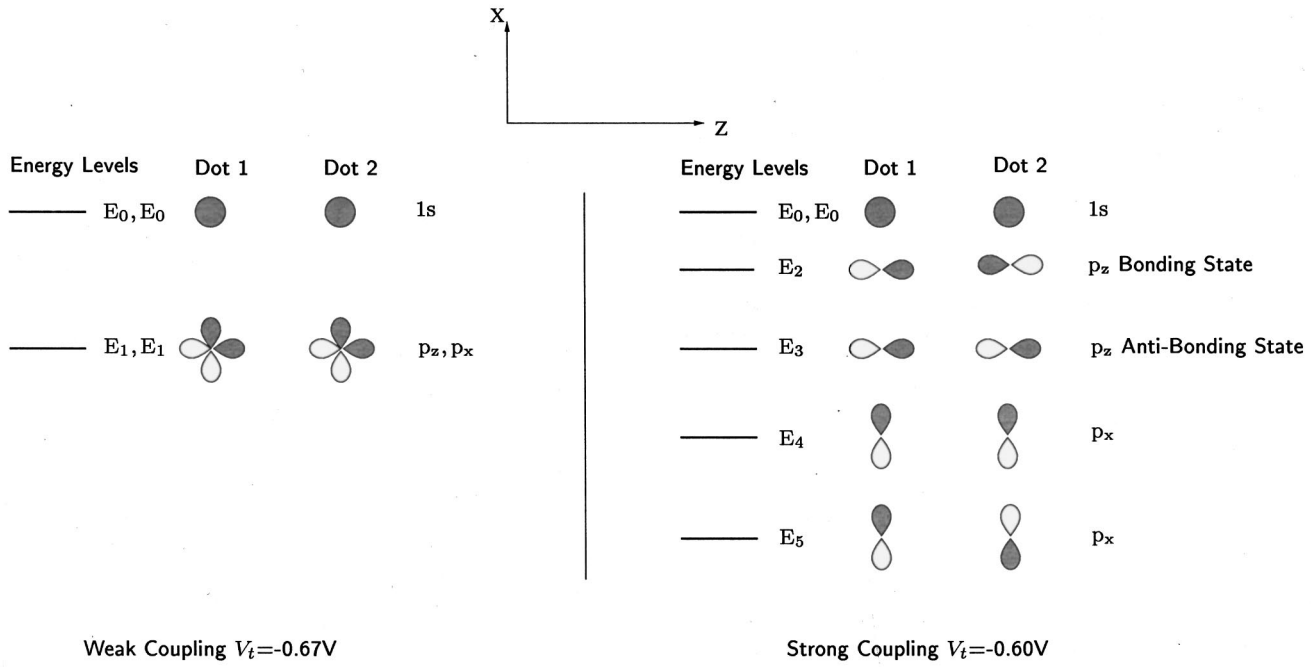

FIG. 3. Schematic representation of the lowest six states in the empty double dot in the weak ($V_t = -0.67$ V) and the strong ($V_t = -0.60$ V) interdot coupling regimes. In the former the p_z and p_x-like states are shown together since they are degenerate within each dot and are decoupled from the corresponding states in the other dot. The reordering of these single-particle states due to increased interdot coupling is also seen. The shaded areas denote the positive portion of the wave functions. Shaded areas indicate a positive value of the wave functions.

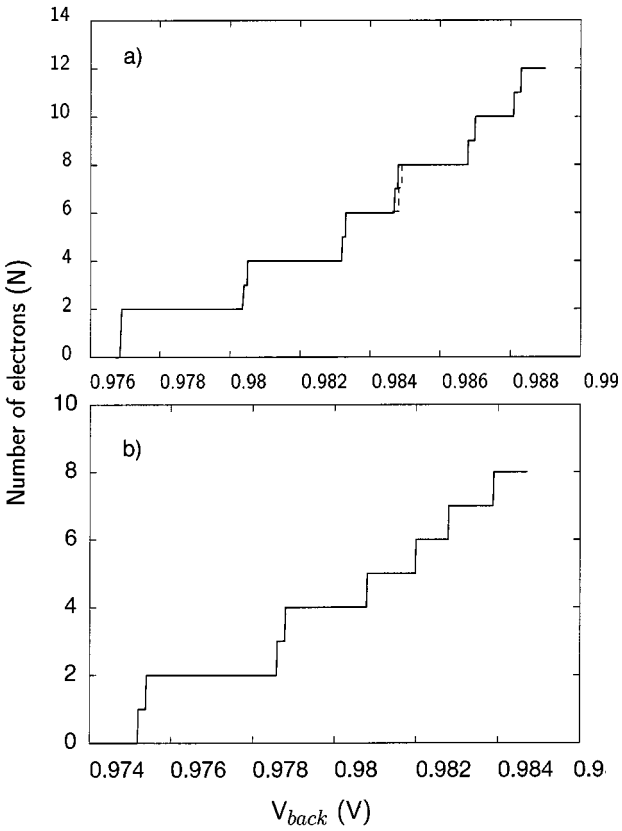

FIG. 4. Coulomb staircase diagram for (a) $V_t = -0.67$ V. The transitions that do not follow Hund's rule are shown in dashed lines. (b) $V_t = -0.60$ V.

functions into the adjacent dot is negligible, and electrostatically since the distance between the two electron distributions is large. The resulting Coulomb repulsion, screened by the high dielectric constant of GaAs ($\epsilon_{\mathrm{GaAs}} = 13.2$), is negligible, or at least weak enough to be overcome by less than 0.1 mV change in V_{back} (which is the minimum increment in V_{back} considered in this work). Thus both dots can be charged simultaneously with an electron each, resulting in N jumping from zero to two. Also, the orientation of the individual spins of the two electrons does not matter; we choose both electrons to be $\uparrow$. This simultaneous (double) charging persists as long as the two dots are isolated. However, as V_{back} is increased to 0.9804 V, when the next charge degeneracy point occurs, even though dots 1 and 2 are identical in all respects only one of them can be charged (with a $\downarrow$ electron) but not both. This is due to the fact that charging, say, dot 1 first increases the total Coulomb repulsion experienced by the incoming electron to dot 2, i.e., electrostatic coupling is established between the dots prior to any appreciable quantum mechanical coupling. Overcoming this repulsion requires a 0.1 mV increment in V_{back} resulting in the termination of double charging, and is evident as a narrow step for $N = 3$. At $V_{\mathrm{back}} = 0.9805$ V, dot 2 also can be charged with a $\downarrow$ electron increasing N to 4. At this point the double-dot is spin unpolarized and the $1s$ ground states of both the dots are completely filled with two electrons ($\uparrow\downarrow$) each.

The next available state for occupation are the p_z and p_x states in each of the dots which are above the ground state by $\simeq$ 1 meV. These states are almost degenerate; the slight splitting of the states caused by the nonisotropicity of the two-dimensional parabolic confining potential in the x-z plane is very small ($\simeq 10^{-6}$ eV). Though either of the two states could be occupied we choose to occupy the p_z state since it is slightly lower in energy than the p_x state by $\simeq 10^{-6}$ eV. Even though the leakage of the p_z state into the interdot barrier is greater than that of the $1s$ state, it is still not coupled to the corresponding p_z state of the adjacent dot to form a bonding state. Consequently, charging of the two p_z states proceeds in the same manner as done for the $N = 2$ to $N = 3$ and $N = 3$ to $N = 4$ electrons. The charging of the dot with the fifth electron occurs at $V_{\mathrm{back}} = 0.9832$ V, where we choose to occupy the p_z state of dot 1 with an $\uparrow$ electron. Subsequent occupation of the p_z state of dot 2 with an $\uparrow$ electron ($N = 5$ to $N = 6$ transition) occurs at $V_{\mathrm{back}} = 0.9833$ V, the 0.1 mV increment in V_{back} being required to overcome the Coulomb repulsion due the fifth electron. It must be noted that the sixth electron occupying p_z state in dot 2 is also of $\uparrow$ spin, which makes the double-dot spin polarized. This configuration is energetically favorable due to the attractive nature of the exchange interaction between the two $\uparrow$ electrons in the p_z states of dots 1 and 2. The unpolarized configuration, where the sixth electron (in the p_z state of dot 2) is of spin $\downarrow$ is less favorable and occurs at a slightly higher value V_{back} (0.98335 V) [dashed curve in Fig. 4(a)]. Likewise, occupying the p_x state of dot 1 with a spin $\uparrow$ electron, thereby increasing N to 7, occurs at a lower voltage than occupying p_x state of dot 1 with a $\downarrow$ electron or completely filling the p_z state of dot 1. This is a demonstration of the familiar Hund's rule whose applicability has been reported in single quantum dots.[29,17] Similarly the eighth electron of $\uparrow$ spin occupies the p_x state of dot 2 at $V_{\mathrm{back}} = 0.9848$ V, requiring a 0.1 mV increment in V_{back} after p_x state in dot 1 has been occupied. As before, this 0.1 mV increase in V_{back} is required to overcome the Coulomb repulsion due to the p_x electron in dot 1. The double dot at this state is spin polarized with 6 $\uparrow$ and 2 $\downarrow$ electrons. The ninth through twelfth electrons (of $\downarrow$ spins) now complete the partially occupied p_x and p_z states in dots 1 and 2, at $V_{\mathrm{back}} = 0.9868$ V, 0.9870 V, 0.9881 V, and 0.9883 V, thereby reverting the double dot to a zero spin state. A feature that is conspicuous over the $N = 9$ to $N = 12$ range is the increasing interaction between the electrons occupying similar single-particle states in the two dots, as evident in the 0.2 mV increment in V_{back} for $N = 9 \rightarrow N = 10$ ($\downarrow$ electrons in the p_z states of dots 1 and 2) and $N = 11 \rightarrow N = 12$ transitions, compared to the 0.1 mV increment for the $N = 5 \rightarrow N = 6$ and $N = 7 \rightarrow N = 8$ transitions. This is a consequence of increasing leakage of the wave functions into the adjacent dot and the center of the charge distributions in the two dots moving towards each other.

Experimental investigations of Waugh *et al.*[5] on arrays of two and three coupled dots confirm our findings. At very low values of the interdot tunneling conductance G_{dd}, they observe the *double charging* effect which is terminated as G_{dd} increases (Fig. 2 in Ref. 5). This is manifested as a splitting of each conductance peak in two (for a double dot) with the separation between them being proportional to the interaction energy δ and increasing with G_{dd}. Another feature that is clear in their results [Figs. 2(a), 2(b), and 2(c) in Ref. 5) is

that even for a fixed G_{dd} the splitting of peak pair increases for larger N. From our investigations we attribute this behavior to the increased electrostatic interaction between the two dots as N increases, as explained in connection with the charging of $N=3$ and $N=4$ electrons. However, as G_{dd} is increased quantum mechanical coupling also contributes to the increased splitting as shall be explained below in relation with Fig. 4(b). For instance, in Fig. 2(a) of Ref. 5, the splitting of the peak is barely discernible about the gate voltage of -1.07 V , but is more pronounced at -1.05–-1.04 V.

Figure 4(b) shows the Coulomb staircase diagram for $V_t=-0.60$ V. The interdot coupling in this case is stronger than in the previous one ($V_t=-0.67$ V), which enhances the leakage of the $1s$ states into the interdot barrier, thereby increasing quantum mechanical as well as electrostatic couplings between the dots. The increase in electrostatic coupling between the dots (quantum-mechanical coupling, although present is still negligible for s states), expectedly, terminates double charging and charging proceeds sequentially from $N=1$ ($V_{\text{back}}=0.9752$ V) to $N=2$ ($V_{\text{back}}=0.9754$ V). The increase in interdot electrostatic interaction is evident from the 0.2 mV increment required to charge dot 2 with $\downarrow$ electron after dot 1 has been charged with an $\uparrow$ electron. This increment in V_{back}, as may be observed from Fig. 4(a), is more than the interaction between the third and fourth electrons that go to complete the $1s$ states in dots 1 and 2 for $V_t=-0.67$ V. The $N=2\rightarrow N=3$ transition occurs at $V_{\text{back}}=0.7586$ V and the $N=3\rightarrow N=4$ transition, at $V_{\text{back}}=0.9788$ V. The four electrons occupy the two $1s$ states in dots 1 and 2. The p_z states which are the lowest available for occupation couple strongly to form symmetric and antisymmetric states akin to *bonding* and *antibonding* states in molecules. A consequence of strong interdot coupling is that for states including p_z and higher states, the double dot appears as a single dot about twice as long along the z direction as along the x direction. These lead to a reordering of states in the eigenenergy spectrum, as the states with increasing n_z (number of nodes along the z direction) get closer and move below the p_x state. Thus, the fifth through eighth electrons occupy sequentially the p_z bonding and antibonding states. This is to be contrasted with the partial filling of p_x and p_z states, for $V_t=-0.67$ V, by fifth through eighth electrons which create a spin polarized state with a net polarization $S=2\hbar$. It is thus clear that an increase in the interdot coupling drives the double dot from a spin polarized to an unpolarized state. Also the Coulomb staircase steps assume a more uniform width for $N>4$ as charging proceeds similar to a single QD.

A complete transformation of the two-dot system into a single large dot requires a de-energizing of the tuning gates, i.e., $V_t=0$ V, a case that has not been considered in this work. However, from the cases considered so far, it can be extrapolated that the separation of the peaks would be maximum and equal to e/C_T, where C_T is the capacitance of the single large dot. This corresponds to the case in Fig. 2(d) in the work of Waugh *et al.*[5]

Figure 5 shows the variation of the spin $\uparrow$ and $\downarrow$ electron densities at the $GaAs/Al_{0.27}Ga_{0.73}As$ interface for $V_t=V-0.60$ V, along the z direction for $N=3$, 5, and 8. Figure 5(a) shows the variation for $N=3$, a spin polarized state with two $\uparrow$ and one $\downarrow$ electrons. The two $\uparrow$ electrons occupy the

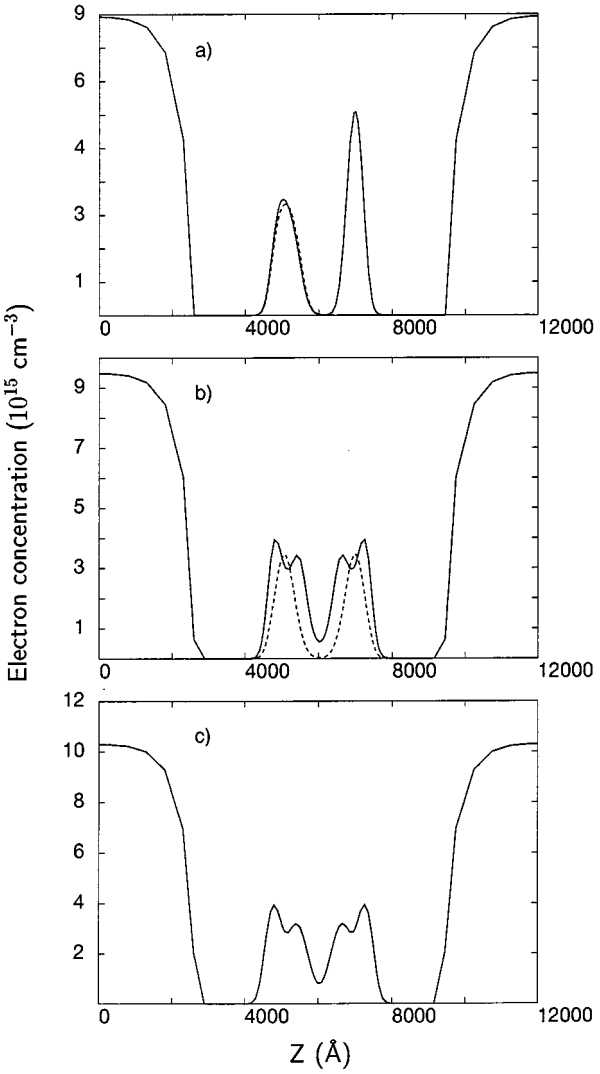

FIG. 5. The variation of the electron spin $\uparrow$ (solid) and $\downarrow$ (dashed) densities at the $GaAs/Al_{0.27}Ga_{0.73}As$ interface along the length of the double dot for (a) $N=3$, $V_{\text{back}}=0.9786$ V, (b) $N=5$, $V_{\text{back}}=0.9808$ V, and (c) $N=8$, $V_{\text{back}}=0.9839$ V. Resolution of spin is confined to the dot region only, i.e., 3000 Å $\leqslant z \leqslant$ 9000 Å. The tuning voltage $V_t=-0.60$ V.

$1s$ sates in dots 1 and 2, respectively, while the $\downarrow$ electron occupies the $1s$ state in dot 1. Consequently, the two electron densities have a $1s$ type distribution in the two dots. The electron densities in the interdot barrier region ($z\simeq 6000$ Å) is small as the coupling of the $1s$ states is weak for this value of V_t. However, as N increases the stronger electron-electron interaction induces a lowering of the barrier, an increase in the leakage of the wave functions, and an increase in the electron densities, in the barrier. This is seen in Fig. 5(b) for $N=5$; the dot is still spin polarized with three $\uparrow$ and two $\downarrow$ electrons. The two $\downarrow$ and two $\uparrow$ electrons occupy the $1s$ states of dot 1 and 2, respectively, while the third $\downarrow$ electron, occupies the p_z-bonding state that gives the jagged profile to the $\downarrow$ electron concentration as seen in the figure. Figure 5(c) shows the variation for $N=8$. This is a spin unpolarized state with four $\uparrow$ and four $\downarrow$ electrons. These fill completely the two $1s$ states in dots A and B and the p_z state. Hence, the two ($\uparrow$ and $\downarrow$) distributions look identical.

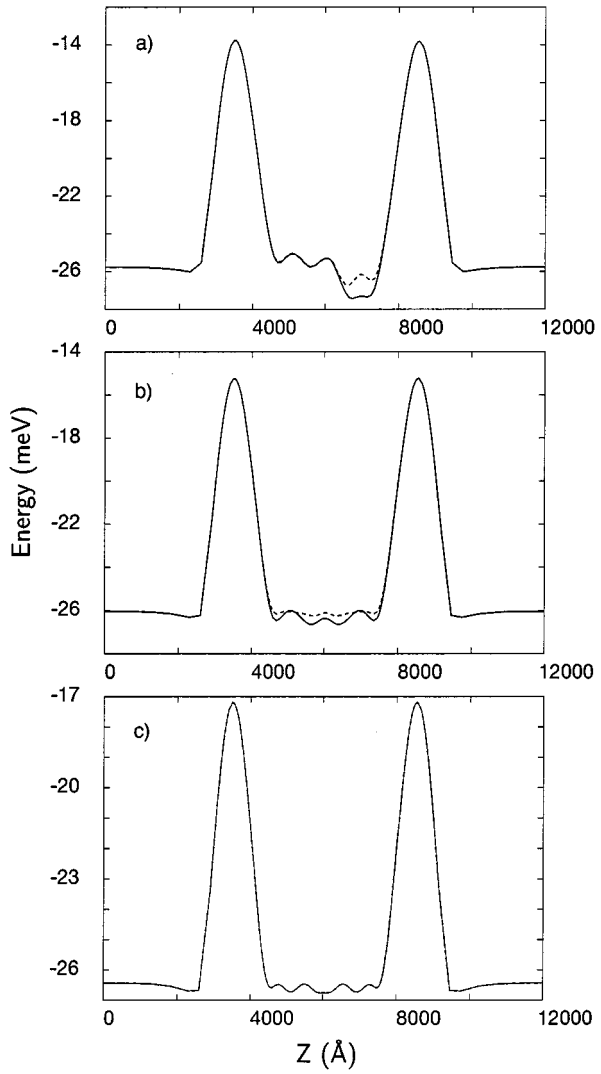

FIG. 6. The variation, along z, of the effective potential energy at the $GaAs/Al_{0.27}Ga_{0.73}As$ interface for the spin $\uparrow$ (solid) and the $\downarrow$ (dashed) electrons for (a) $N=3$, $V_{back}=0.9786$ V, (b) $N=5$, $V_{back}=0.9808$ V, and (c) $N=8$, $V_{back}=0.9839$ V. The tuning voltage $V_t=-0.60$ V.

It is also seen in Fig. 5 that the peak electron densities decrease with increasing N. This apparent anomaly is caused by an increase in the volume of the dot that accompanies an increase in N. As a result, the width of the electron density peaks broadens while the peaks lower which is seen more clearly where the electron density (along the y direction) peaks about 400 Å away from (not shown) rather than at the heterointerface.

Figure 6 shows the variation of the effective potential energy for the up and down spin electrons at the $GaAs/Al_{0.27}Ga_{0.73}As$ interface for $V_t=-0.60$ V, along the z direction, for $N=3$, 5, and 8. The profile for $N=0$ is similar to that shown in Fig. 2 but the height of the interdot barrier is lower at 3 meV. In a spin polarized state the effective potential for $\uparrow$ electrons is different from that for the $\downarrow$ electrons, since $\mu_{xc}(\mathbf{r})$ for each of them is different. In the $N=3$ case shown in Fig. 6(a) the higher $\uparrow$ density leads to a larger $\mu_{xc}^{\uparrow}(\mathbf{r})$, which, being attractive, lowers the net electron-electron interaction energy. This also leads to the interdot barrier seen by the $\uparrow$ electrons to be slightly higher than that seen by the $\downarrow$ ones. When N increases to 5, as in Fig. 6(b), the large $\uparrow$ density in the barrier region and the resulting $\mu_{xc}^{\uparrow}(\mathbf{r})$ leads to a drastic reduction in the barrier height. The potential energy profile for the $\uparrow$ electrons then resembles a single large dot, instead of a coupled dot. In contrast, for the $\downarrow$ electrons whose density in the barrier is small the potential energy is characteristic of a coupled-dot system. With a further increase in N to 8 (four each of $\uparrow$ and $\downarrow$ electrons), as in Fig. 6(c), the profiles for the $\uparrow$ and $\downarrow$ electrons are identical. The interdot barrier separation is extremely small and is barely noticeable in the figure. A feature that is evident in Figs. 6, typical of electrostatically defined dots, is the decrease in confinement with increasing N. The effective barrier at the source and drain ends decreases from $\simeq$ 15 meV for $N=0$ to about 9 meV for $N=8$.

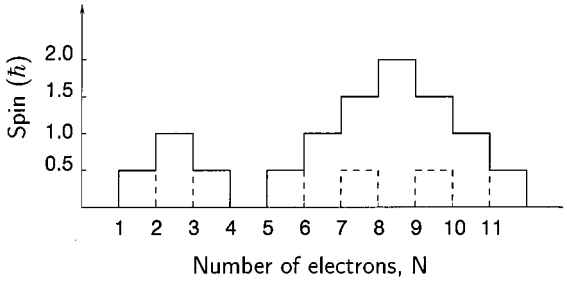

FIG. 7. Variation of the total electron spin S in the double dot with N for $V_t=-0.67$ V (solid line) $V_t=-0.60$ V (dashed line).

The variation of interdot coupling by varying V_t is comparable to the vibration of a diatomic molecule. Weak coupling (a large negative V_t) is comparable to the situation wherein the distance between the atoms is large, and strong coupling when the distance is a minimum. Thus by varying V_t the level crossing as a function of separation between the artificial atoms in the molecule can be studied. From the Coulomb staircase diagrams of Figs. 4(a) and 4(b) and the ensuing discussions it is seen that a lowering of the interdot barrier results in a reordering of the single-particle levels, thereby transforming the doubledot (for $N=8$) from a spin polarized to an unpolarized state. The variation of total spin with the number of electrons in the dot in the weak ($V_t=-0.67$ V) and strong ($V_t=-0.60$ V) coupling regimes is illustrated in Fig. 7. For weak coupling the total spin of the dot increases in steps of $\hbar/2$ between $N=5$ and $N=8$ as the p_x and p_z states in dots 1 and 2 get charged with an electron each of $\uparrow$ spin, which is an illustration of the familiar Hund's rule in atomic shell filling. For strong coupling such a spin polarization of the dot is precluded by a lifting of degeneracy of the p_x and p_z states, and the total spin is never greater than $\hbar/2$. We would like to draw attention to the fact that for $V_t=-0.67$ V the total spin is seen to be $\hbar$ for $N=2$ (Fig. 7). This, however, does not imply that the double dot is spin polarized, but rather that since the dots are electrostatically decoupled the spins of the two electrons are not correlated in any way. Though in reality there may be a weak interaction between the two electrons, such an interaction is not observable within the resolution of our model, and our choice of the two electrons being of parallel spin is incidental.

V. CONCLUSIONS

We have investigated the electronic properties of a double-dot system by considering a spin dependent model under the local spin density approximation (LSDA). We observe that an increase in the interdot interaction caused by an increase in the coupling strength leads to a splitting of the conductance peaks. We also observe that for a fixed interdot coupling strength, an increase in the number of electrons in the system leads to an increase in the separation between the split peaks due to an increase in electrostatic coupling; these are in good agreement with experiments. Furthermore, we have demonstrated the possibility of changing the total spin of the double-dot system by varying the interdot coupling strength. For an eight electron system, we observe that in the weak interdot tunneling regime the system prefers a spin polarized ground state with four electrons occupying degenerate single particle states; but as the tunneling strength increases the reordering of energy levels removes the degeneracy and the system switches to a spin unpolarized state.

ACKNOWLEDGMENTS

We would like to thank L. Fonseca and I. H. Lee for valuable discussions, and Y. H. Kim for making available the LSDA subroutines. This work was supported by NSF Grant No. ECS 95-09751. One of us (S.N.) would like to acknowledge support from the Beckman Institute.

[1] K. Imamura, Y. Sugiyama, Y. Nakata, S. Muto, and N. Yokoyama. Jpn. J. Appl. Phys. **34**, 1445 (1995).
[2] S. Fafard, K. Hinzer, S. Raymond, M. Dion, J. McCaffrey, Y. Feng, and S. Charbonneau. Science **274**, 1350 (1996).
[3] G. W. Bryant, Phys. Rev. B **48**, 8024 (1993).
[4] R. H. Blick, D. Pfannkuche, R. J. Haug, K. v. Klitzing, and K. Eberl, Phys. Rev. Lett. **80**, 4032 (1998).
[5] F. R. Waugh, M. J. Berry, D. J. Mar, R. M. Westervelt, K. L. Campman, and A. C. Gossard, Phys. Rev. Lett. **75**, 705 (1995).
[6] L. Kouwenhoven, Science **268**, 1440 (1995).
[7] R. H. Blick, R. J. Haug, J. Weis, D. Pfannkuche, K. v. Klitzing, and K. Eberl, Phys. Rev. B **53**, 7899 (1996).
[8] R. J. Haugh, R. H. Blick, and T. Schmidt, Physica B **212**, 207 (1995).
[9] N. C. van der Vaart, S. F. Godijn, Y. v. Nazarov, C. J. P. M. Harmans, J. E. Mooij, L. W. Molenkamp, and C. T. Foxon, Phys. Rev. Lett. **74**, 4702 (1995).
[10] K. A. Matveev, L. I. Glazman, and H. U. Baranger, Phys. Rev. B **53**, 1034 (1996).
[11] I. M. Ruzin, V. Chandrashekar, E. I. Levin, and L. I. Glazman, Phys. Rev. B **45**, 13 469 (1992).
[12] C. A. Stafford and S. Das Sharma, Phys. Rev. Lett. **72**, 3590 (1994).
[13] G. Klimeck, G. Chen, and S. Datta, Phys. Rev. B **50**, 2316 (1994).
[14] J. M. Golden and B. I. Harpen, Phys. Rev. B **53**, 3893 (1996).
[15] A. Kumar, S. E. Laux, and F. Stern, Phys. Rev. B **42**, 5166 (1990).
[16] S. Nagaraja, P. Matagne, J. P. Leburton, Y. H. Kim, and R. M. Martin, Phys. Rev. B **56**, 15 572 (1997).
[17] I. H. Lee, V. Rao, R. M. Martin, and J. P. Leburton, Phys. Rev. B **57**, 9035 (1998).
[18] L. R. C. Fonseca, J. L. Jimenez, J. P. Leburton, and R. M. Martin, Phys. Rev. B **57**, 4017 (1998).
[19] A. Wojs and P. Hawrylak, Phys. Rev. B **53**, 10 841 (1996).
[20] M. Koskinen, M. Manninen, and S. M. Rieman, Phys. Rev. Lett. **79**, 1389 (1997).
[21] R. O. Jones and O. Gunnarsson, Rev. Mod. Phys. **61**, 689 (1989).
[22] D. Jovanovic and J. P. Leburton, Phys. Rev. B **49**, 7474 (1994).
[23] M. Stopa, Phys. Rev. B **54**, 13 767 (1996).
[24] M. Macucci, K. Hess, and G. J. Iafrate, Phys. Rev. B **55**, R4879 (1997).
[25] J. P. Perdew and Z. Zunger, Phys. Rev. B **23**, 5048 (1981).
[26] J. P. Perdew and Y. Wang, Phys. Rev. B **45**, 13 244 (1992).
[27] S. M. Sze, *Physics of Semiconductor Devices* (Wiley, New York, 1981).
[28] J. C. Slater, *Quantum Theory of Molecules and Solids* (McGraw-Hill, New York, 1963).
[29] S. Tarucha, D. G. Austing, T. Honda, R. J. van der Hage, and L. P. Kouwenhoven, Phys. Rev. Lett. **77**, 3613 (1996).